DALTON
FULL PAPER

Solvent-dependent assembly of mixed-metal *N,N′*-diphenylbenzamidinate oxide and alkoxide complexes

Andrew D. Bond, David J. Linton, Paul Schooler and Andrew E. H. Wheatley *

Department of Chemistry, University of Cambridge, Lensfield Road, Cambridge, UK CB2 1EW

Received 21st May 2001, Accepted 24th August 2001
First published as an Advance Article on the web 15th October 2001

The sequential reaction of $ZnMe_2$ with *N,N′*-diphenylbenzamidine (= HAm **10**), $LiBu^t$ and molecular oxygen affords various lithium triorganozincate species, the identity of which depend upon the solvent conditions used. In the presence of THF, the isolated product is a dimer $[THF{\cdot}Li(Me)OZnAm_2]_2$ **12**, wherein oxygen has formally inserted into the Zn–C bond of a $MeZnAm_2^-$ anion. Compound **12** is based on a $(ZnO)_2$ ring core with exocyclic alkali metal centres. In the absence of donor solvent, crystals are obtained of both the pseudo-octahedral oxide-encapsulation complex $(\mu_6\text{-}O)(Li_2ZnAm_3)_2$ **13** and the heterobimetallic alkoxide polymer $[(LiOBu^t)(MeZnOBu^t)_3]_\infty$ **14**. The structures of **12**–**14** all suggest a predilection for μ_3 oxygen-capped triangulated metal arrays in oxophilic mixed Li–Zn systems.

Introduction

Heterobimetallic systems incorporating lithium are responsible for many chemical transformations whose selectivities differ from those observed if either parent single-metal species is used instead.[1,2] In the field of mixed Li–Zn chemistry, for example, lithium silyl(dialkyl)zincates[3] have been reported to achieve conjugate addition to α,β-unsaturated ketones;[4] this contrasts with the well documented 1,2-addition[5] of organolithium reagents across such substrates.[6] Moreover, lithium triorganozincates have been employed in conjunction with propargylic species to afford α,γ-disubstituted propargyles or allenes,[7] with aryl halides to effect halogen–zinc exchange,[8] or with 1,1-dihalocyclopropyls and 1-haloalkenylzincates to afford metal carbenoids.[9] Recently, effort has also gone into realising the synthetic potential[10] of dilithium tetraorganozincate complexes of the type Li_2ZnMe_3R (R = Me, CN, SCN).[11]

A survey of the literature[2] demonstrates, however, that the structural chemistry of lithium organozincates is not well understood. Although $(Li^+)_2ZnMe_4^{2-}$ has been characterised in the solid state,[12] ion-separated homoleptic triorganozincates (Li^+ ZnR_3^-) are more common. Mixed coordination of the Group 1 metal centre is observed in $Et_2O{\cdot}TMEDA{\cdot}Li^+$ $Zn[C(H)(SiMe_3)_2]_3^-$ (TMEDA = *N,N,N′,N′*-tetramethylethylenediamine)[13] while two molecules of TMEDA encapsulate the Li^+ ions in the salts of the heteroleptic zincate ions $Zn(Me)_2C(H)(Ph)SiMe_3^-$ and $Zn(Me)[C(H)(Ph)SiMe_3]_2^-$,[14] and two equivalents of 1,3,5-trimethyl-1,3,5-triazine (= L) envelope the alkali metal centre in $(L)_2{\cdot}Li^+$ $Zn(Me)\{C(H)[Si(Me)_2C(H)_2]_2SiMe_2\}_2^-$.[15] The Li(μ-C)Zn motif has been noted in ion-bonded lithium zincate chemistry, with monomeric $THF{\cdot}LiZn[2\text{-}(Me_2NCH_2)C_6H_4]_3$ revealing a mono-aryl bridge between the two metal centres.[16] Moreover, $Li(\mu\text{-}C)_2Zn$ motifs dominate the structural chemistry of dilithium tetraorganozincate complexes with $Li(\mu\text{-}C)_2Zn(\mu\text{-}C)_2Li$ spirocyclic motifs noted for $L{\cdot}Li_2Zn[(CH_2)_4]_2$,[17] $L{\cdot}Li_2Zn(C{\equiv}CPh)_4$,[18] $L{\cdot}Li_2Zn[(CH_2SiMe_2)_2]_2$,[19] (L = TMEDA), $Li_2Zn[2\text{-}(Me_2NCH_2)C_6H_4]_4$[16] and $\{Li_2Zn[O_2C(CH)_2Me]_4\}_\infty$.[20] The inclusion of electron rich heteroatoms in the zinc-bonded organic residues has also been noted and has led to the isolation and characterisation of ion-associated species such as $Li(\mu\text{-}N)Zn$-bridged $L{\cdot}LiZn(CH_2SiMe_3)_2N(SiMe_3)_2$ (L = 1,3,5-trimethyl-1,3,5-triazine)[15] and $Li(\mu\text{-}N)_2Zn$-bridged $LiZn(HMDS)_2Me$ (HMDS = 1,1,1,3,3,3-hexamethyldisilazide).[21]

Reports exist of the incorporation of oxygen by mixed s-block metal compounds[22–24] and, more recently, Group 1–Group 12 systems.[21] However, advances have also been made in our understanding of the controlled oxygenation of mixed s-/p-block species. In seeking to extend recent work on the selective oxygenation of lithium aluminates[25] we have reported that the sequential reaction of $ZnMe_2$ with a 2-pyridylamine [HN(2-C_5H_4N)R, R = Ph **1**, 3,5-xy **2** (xy = xylyl), 2,6-xy **3**, Me **4**], $LiBu^t$ and thereafter with air (pre-dried over P_2O_5) affords a wide variety of lithium zincate motifs which, in turn, reveal a diversity of oxo-capture modes in the solid state.[26,27] Compound **1** yields both the dimer of $THF{\cdot}Li(Me)OZn[N(2\text{-}C_5H_4N)Ph]_2$ **5**, in which oxygen has formally inserted into the Zn–C bond of a $MeZn[N(2\text{-}C_5H_4N)Ph]_2^-$ anion, and trigonal Li_2Zn bis(OBu^t)-capped $(THF{\cdot}Li)_2(\mu_3\text{-}OBu^t)_2Zn[N(2\text{-}C_5H_4N)Ph]_2$ **6**. The employment of **2** results in the isolation and structural characterisation of an analogue of **5** (**7**), while the use of the sterically-congested 2,6-xylyl isomer, **3**, gives the heterobimetallic pseudo-cubic dimer $[THF{\cdot}Li(Bu^t)OZn(OBu^t)Me]_2$ **8** in which labile Zn–C(Me) bonds are retained. Less sterically-demanding amine **4** affords the oxide-encapsulation product $Bu^t(\mu_3\text{-}O)Li_3(\mu_6\text{-}O)Zn_3[N(2\text{-}C_5H_4N)Me]_6$ **9**, in which concomitant oxo-insertion into a Li–C interaction results in (OBu^t)-capping of an unusual[28] type of *fac*-isomeric $(\mu_6\text{-}O)M_3M'_3$ octahedron.[26]

We report here on the extension of oxygen-capture chemistry in mixed Li–Zn systems from those containing 2-pyridylamide groups[26,27] to analogous reaction mixtures incorporating a benzamidinate ligand.[29] Specifically, we discuss the variability and selectivity of chalcogen capture revealed on oxygenation of the heterobimetallic systems which result from the sequential reaction of $ZnMe_2$ with *N,N′*-diphenylbenzamidine, PhN(H)C(Ph)=NPh (HAm) **10**, and $LiBu^t$.

Results and discussion

Reaction of a toluene solution of **10** with $ZnMe_2$ results in the facile evolution of CH_4. The subsequent addition of $LiBu^t$ affords a solution which, on storage at ambient temperature, yields a single microcrystalline material, **11**, which multinuclear NMR spectroscopy, elemental analysis and melting point suggest to be the simple lithium amidinate $(LiAm)_n$[30]—a species hitherto crystallographically characterised only as a monomeric

DOI: 10.1039/b104444n

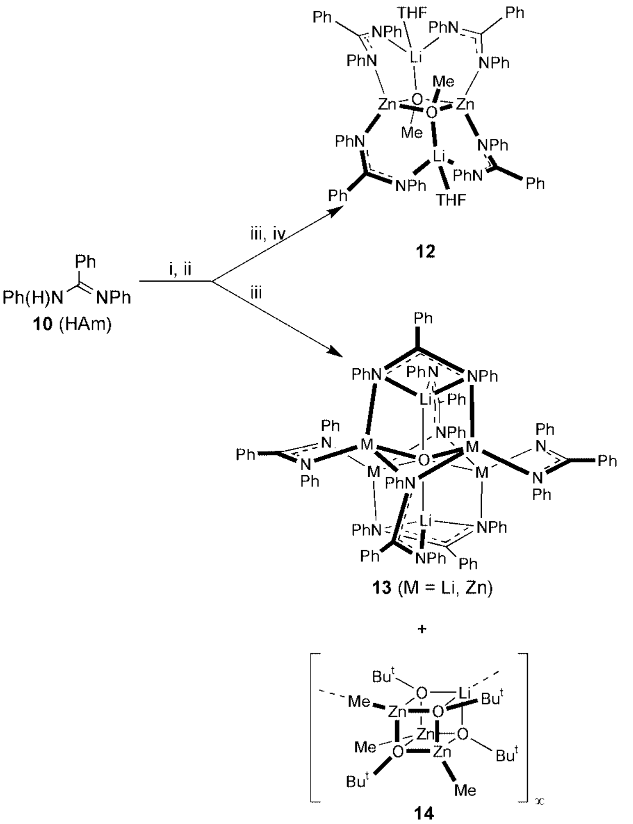

Scheme 1 Reagents and conditions: i, $ZnMe_2$–toluene; ii, $LiBu^t$–pentane; iii, O_2; iv, THF.

complex with TMEDA or PMDETA (= *N,N,N′,N″,N″*-pentamethyldiethylenetriamine) and as a dimer with HMPA (= hexamethylphosphoramide).[30] The introduction of molecular oxygen to the **10**–$ZnMe_2$–$LiBu^t$ reaction mixture immediately after it reaches room temperature affords a slurry which dissolves either on addition of THF or of further toluene (see below). The solution yielded by THF application deposits colourless crystals of **12** on storage at room temperature (Scheme 1). This product is revealed by X-ray crystallography to have a structure analogous to the recently reported oxygenated dimers of THF·Li(Me)OZn[N(2-C_5H_4N)R]$_2$ (R = Ph **5**, 3,5-xy **7**).[27] Whereas it has been noted that mixed Li–Y,[31] Li–Yb,[32] Li–Sm,[33] Li–V[34] and, perhaps more importantly, Li–Mn[35] systems are capable of abstracting the oxygen from THF, to our knowledge this behaviour has not been reported for Li–Zn systems. Moreover, we have recently established that complexes of the type THF·Li(R)Zn[N(2-C_5H_4N)Ph]$_2$ (R = alkyl) (which logically represent precursors to species akin to **12**) are isolable from THF-containing media.[36] Thus, taken in conjunction with the synthesis and characterisation of **13** and **14** from non-donor media (see below), the ability of **11** and **12** to be isolated from systems of this type suggests that reaction in the latter case has occurred between supplied molecular oxygen and a lithium zincate complex which in the former case eliminated thermodynamically favoured **11**—perhaps because of the influence of THF (see below). While ongoing mechanistic studies have, as yet, failed to elucidate whether the precursor to **12** formally incorporates a $MeZnAm_2^-$ anion it is clear that empirically an oxygen atom has inserted into the single, labile Zn–C bond of such a moiety. As for **5** and **7**, the asymmetric unit of this product contains half of the dimeric aggregate, half a toluene molecule and a single, disordered lattice THF molecule. The structure, built around a planar $(ZnO)_2$ ring [mean Zn–O = 2.004 Å, O–Zn–O = 84.74(9)°, Zn–O–Zn = 95.26(9)°], renders each zinc centre tetrahedral (Fig. 1 and Table 1). The alkali metal centres are *anti*-disposed about the $(ZnO)_2$ metallocycle, interacting with it *via* the core O-centres [Li1–O1 = 1.936(6) Å]. Each Li^+ ion is also electronically supported by the coordination of two pyridyl N-centres (mean Li–N = 2.102 Å) such that each $\mathrm{N}\overset{\cdots}{-}\mathrm{C}\overset{\cdots}{-}\mathrm{N}$ fragment spans a Li–O–Zn moiety and affords an LiO-edge-fused pair of MOM′NCN 6-membered rings. The observation of these structural details for **12** goes some way to establishing that the $(ZnO)_2$ ring-centred structure type noted for 2-pyridylamide complexes **5** and **7**[27] is, in fact, general for oxophilic Li–Zn systems containing $\mathrm{N}\overset{\cdots}{-}\mathrm{C}\overset{\cdots}{-}\mathrm{N}$-based ligands.

Table 1 Selected bond lengths (Å) and angles (°) for dimeric **12**

Li1–O1	1.936(6)	Zn1–N4	1.982(3)
Li1–O2	2.024(6)	O1–C39	1.438(4)
Li1–N2	2.087(6)	N1–C38	1.357(4)
Li1–N3A	2.117(6)	N2–C38	1.316(5)
Zn1–O1	2.003(2)	N3–C19	1.327(4)
Zn1–O1A	2.004(2)	N4–C19	1.342(4)
Zn1–N1	1.980(3)		
Li1–O1–C39	114.1(3)	O1–Zn1–N1	115.15(11)
Li1–O1–Zn1	105.6(2)	O1–Zn1–N4	112.61(10)
Li1–N2–C38	128.9(3)	Zn1–O1–Zn1A	95.26(9)
Li1–N3A–C19A	119.3(3)	Zn1–N1–C38	124.3(2)
O1–Li1–O2	105.8(3)	Zn1–N4–C19	121.6(2)
O1–Li1–N2	108.9(3)	N1–C38–N2	119.9(3)
O1–Li1–N3A	103.5(3)	N3–C19–N4	118.8(3)
O1–Zn1–O1A	84.74(9)		

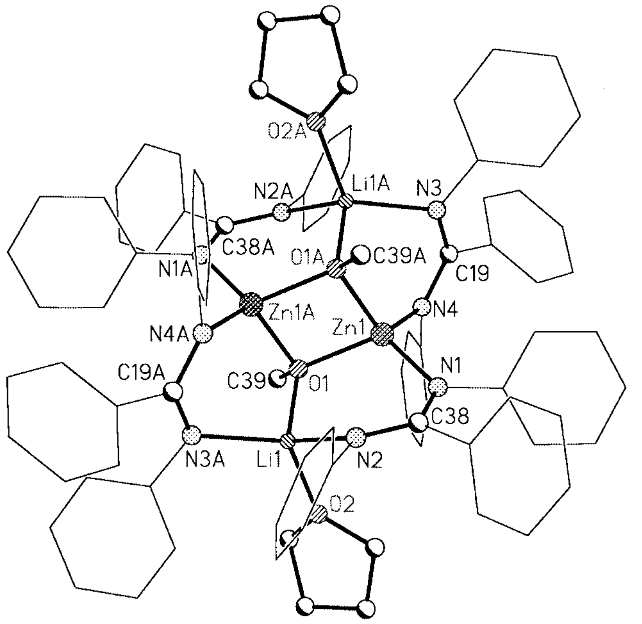

Fig. 1 Molecular structure of dimeric THF-solvate **12**; hydrogen atoms and lattice toluene and THF molecules omitted for clarity.

The employment of a non-donor medium for the reaction described above—that is, affecting dissolution not by addition of THF but by that of further toluene—has enabled the isolation and characterisation of a new heterobimetallic oxide-encapsulation cluster, **13**, and of a metal alkoxide polymer, **14**. Thus, dissolution is now followed by the deposition of a mixture of both cubes and needles (Scheme 1). These can be mechanically separated for the purposes of analysis, although NMR spectroscopy reveals a small amount of cross-contamination in the case of **13** and this is reflected in the elemental analyses of that compound. X-Ray crystallography of the former type of crystal reveals that this product (**13**) of reaction in the absence of external Lewis bases is (μ_6-O)(Li_2ZnAm_3)$_2$ (Fig. 2) for which formulation there are two lattice toluene molecules. The molecular unit displays 2-fold rotational symmetry, with the 2-fold axis (0, *y*,¼) passing through O1 and the formyl C-centres C49 and C60. Of the three crystallographically-independent metal sites, one is wholly occupied by Li^+ (Li3) while the other two are disordered with refined site occupancies 42%Li : 58%Zn

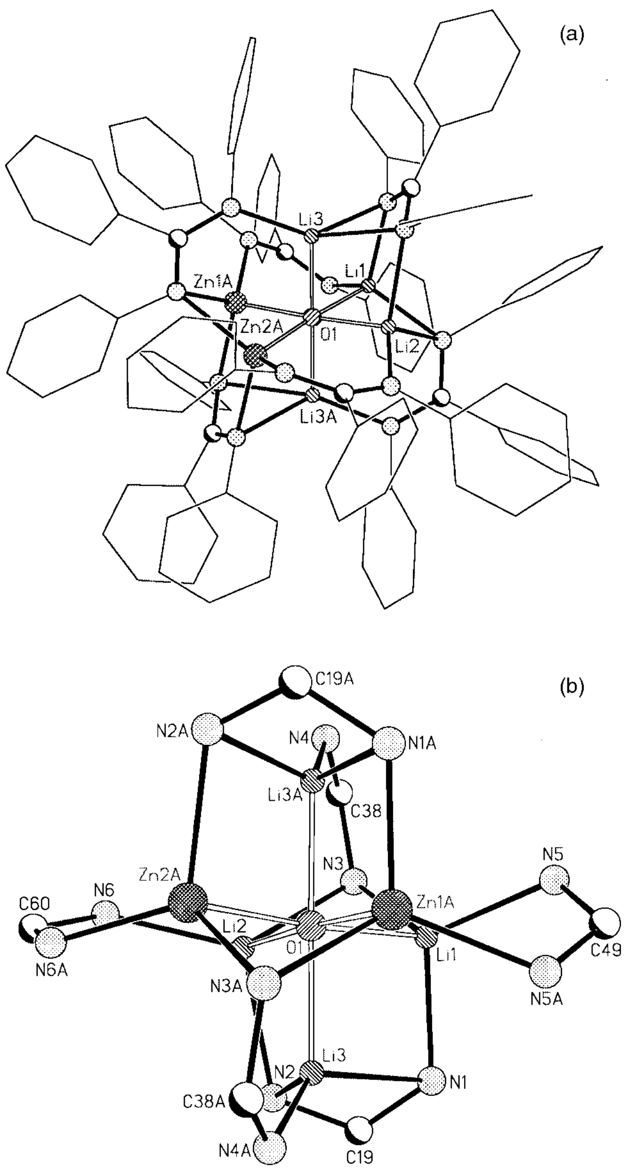

Fig. 2 (a) Molecular structure of Li_4Zn_2-based oxide-encapsulation complex **13**; disorder in the metal centres, hydrogen atoms and lattice toluene molecules omitted for clarity. (b) The core of **13**.

and 58%Li : 42%Zn for Li1/Zn1 and Li2/Zn2, respectively—an arrangement which satisfies the requirement for charge balance in the cluster. Thus, the M_6O^{6+} cluster core consists of an Li_2Zn_2 (= M_4) plane in which there is positional disorder of the metal ions, with Li^+ ions in the axial positions of the distorted octahedron. Fig. 2 shows one possible arrangement of this octahedron. It should be noted that the refined site occupancy factors reflect the metal populations *averaged over the whole lattice*. Furthermore, the amidinate ligands coordinating this octahedron will adopt slightly different orientations based on the exact arrangement of the metal ions, such that the ligand positions also reflect an average over the whole lattice. This subtle positional disorder is reflected by the displacement parameters of the carbon centres, the effect being most pronounced at the extremities of the ligands that chelate the M_4-plane (*e.g.* C52–C54 in Fig. 3).

The Li–O and Zn–O bond distances suggest that the four metal centres in the M_4 plane are less strongly bonded to encapsulated O1 than is Li3 [Li1/Zn1–O1 = 2.029(2) Å, Li2/Zn2–O1 = 1.957(2) Å, *cf.* Li3–O1 = 1.915(7) Å] such that the cluster could be considered to contain a near linear [Li3–O1–Li3A = 178.9(5)°] lithium oxide moiety. Moreover, the metal centres in the M_4 plane display significantly different bonding

Table 2 Selected bond lengths (Å) and angles (°) for distorted octahedral **13**

Li1–O1	2.029(2)	Li3–N1	2.377(8)
Li1–N1	2.023(3)	Li3–N2	2.140(8)
Li1–N3	2.145(4)	Li3–N4A	1.981(8)
Li1–N5	2.054(3)	N1–C19	1.338(5)
Li2–O1	1.957(2)	N2–C19	1.335(5)
Li2–N2	2.174(3)	N3–C38	1.345(6)
Li2–N3	2.279(4)	N4–C38	1.318(6)
Li2–N6	2.025(3)	N5–C49	1.333(4)
Li3–O1	1.915(7)	N6–C60	1.330(4)
Li1–O1–Zn1A	98.33(14)	O1–Li3–N2	100.8(3)
Li1–O1–Li2	81.75(3)	O1–Li3–N4A	115.9(4)
Li1–O1–Li3	86.9(2)	Li1–N3–Li2	72.21(11)
Li1–O1–Li3A	92.4(2)	Li1–N1–C19	124.2(3)
Li2–O1–Li3	84.0(2)	Li1–N3–C38	119.7(3)
Li2–O1–Li3A	96.7(2)	Li1–N5–C49	119.1(3)
Li2–O1–Zn2A	98.39(15)	Li2–N2–C19	122.3(3)
Li3–O1–Li3A	178.9(5)	Li2–N6–C60	125.2(3)
O1–Li1–N1	102.38(10)	N1–Li3–N2	60.8(2)
O1–Li1–N3	95.97(14)	N1–Li3–N4A	139.3(4)
O1–Li1–N5	110.42(13)	N2–Li3–N4A	131.5(4)
O1–Li3–N1	94.1(3)	N1–C19–N2	118.4(4)
O1–Li2–N2	98.28(10)	N5–C49–N5A	118.2(5)
O1–Li2–N3	93.84(13)	N6–C60–N6A	120.1(5)
O1–Li2–N6	118.32(13)		

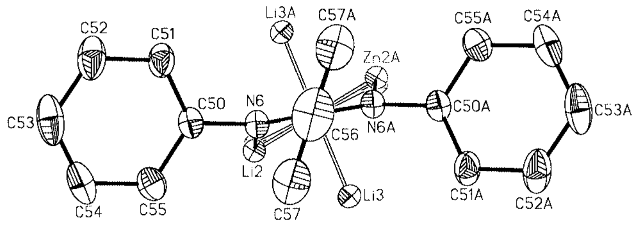

Fig. 3 Thermal ellipsoid plot (drawn at 30% probability) of **13** viewed along its C49–C60 axis; hydrogen atoms omitted for clarity.

interactions with O^{2-} depending on whether the metals interact with N5 or N6, belonging to two different amidinate ions. These two ligands straddle two metal centres and as such bridge opposing edges of the distorted octahedral core. The amidinate groups display two different mean orientations with respect to the M_4 plane—the averaged (N5C49N5A)–M_4 and (N6C60-N6A)–M_4 torsion angles being 40.0° and 18.5°, respectively. The remaining four amidinate ligands each bond to three metal ions and cap octahedral faces in two distinct ways. The first ligand type bonds through one N-centre (N3A) to each of two metal ions in the M_4 plane (*e.g.* Zn1A and Zn2A in Fig. 2) while interacting with Li3 using its other N-centre (N4A). The second capping mode requires that N1 and N2 interact with one metal centre in the M_4 plane while chelating Li3. The multiplicity of different binding modes between the M_6O^{6+} cluster core and the amidinate periphery gives rise to significant differences in metal–nitrogen bond lengths (Table 2).

The bonding patterns observed in **12** and **13** can be correlated with the structural chemistry recently reported for the selectively oxygenated 2-pyridylamide complexes **5**–**9**. It is noteworthy that the arrangement of metal centres in **12** means that, like these earlier species, it too can be interpreted in terms of triangulated $LiZn_2$ arrays (Li1Zn1Zn1A and Li1AZn1Zn1A) each of which is capped by an *in situ* generated alkoxy moiety (O1C39 and its symmetry equivalent, respectively). The approximate equivalence of Li–X and Zn–X (X = N, O) bond distances leads to the interconvertability of lithium and zinc in such motifs. Hence, **8** and **9** empirically contain both $LiZn_2$ and Li_2Zn arrangements.[27] In a similar vein, compound **13** displays two Li_2Zn triangles. The first of these triangles comprises Li3 along with Li1A/Zn1A and Li2A/Zn2A, while the second utilises Li3A, Li1/Zn1 and Li2/Zn2. Such a model predicts that the

Table 3 Selected bond lengths (Å) and angles (°) for **14**

Li1A–O1	2.028(3)	Zn3–O1	2.058(4)
Li1A–O3	2.024(3)	Zn3–O2	2.064(3)
Li1A–O2A	2.078(3)	Zn1–C1	2.118(1)
Zn2–O2	2.068(3)	Zn2–C12	1.983(6)
Zn2–O3	2.061(4)	Zn3–C13	1.968(7)
Li1A–O1–Zn1	91.34(15)	O1–Li1A–O3	88.25(11)
Li1A–O3–Zn1	91.54(15)	O1–Li1A–O2A	85.86(13)
Zn1–O2–Zn2	93.49(11)	O2–Zn1–O3	85.82(13)
Zn1–O2–Zn3	93.41(11)	O2–Zn2–O2A	84.51(15)
Zn2–O2–Zn3	95.19(11)	O2–Zn2–O3	85.16(10)
Zn1–O1–Zn3	95.08(13)	O1–Zn3–O2	85.46(10)
Zn1–O3–Zn2	95.31(12)	O2–Zn3–O2A	84.72(15)

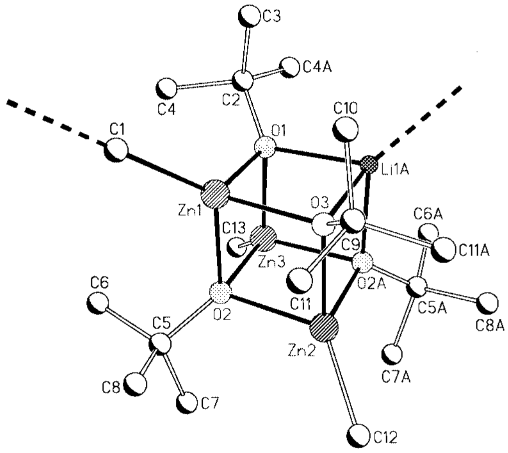

Fig. 4 Molecular structure of polymeric **14**; minor Bu^t disorder and hydrogen atoms omitted for clarity.

two amidinate ligands which chelate the M_4 plane are, in fact, employed only in holding the two triangles together about central O1. Meanwhile, the actions of the remaining four ligands can be interpreted in the context of dimeric **12** wherein amidinate groups bridge the Li···Zn divides that define the *edges* of triangulated metal arrays.

While examples of oxide-trapping species with various coordination geometries[22,23,37,38] at the chalcogenide centre resulting from the oxophilic properties of lithiated systems are known, the majority of such lithium-containing complexes have been based on homometallic Li_6O^{4+} octahedra.[39,40] Examples of Li-containing heterobimetallic octahedra which μ_6-envelope isolated O^{2-} have hitherto been limited to just $[RuH(SiHPh_2)(CO)X_2]_2 \cdot [Li_2Ru_4OCl_8X_4]$ (X = PBu^t_2Me),[41] $Li_3(\mu_6\text{-}O)Ba_3(\mu_6\text{-}O)[(THF)_3 \cdot Ba_3](O^tBu)_{11}$,[28] and *fac*-$Bu^t(\mu_3\text{-}O)Li_3(\mu_6\text{-}O)Zn_3[N(2\text{-}C_5H_4N)Me]_6$ **9**.[27] Other metals and ratios have also been noted, *e.g.* MM'_5 ($TiMo_5$)[42] and $M_2M'_4$ (Ba_2Y_4,[43] Bi_2Na_4,[44] Sb_2Na_4,[45] Sb_2K_4,[46] Zr_2Co_4[47] and Zr_2K_4[48]).

The isolation and characterisation of heterobimetallic **13** is of particular consequence for our view of the formation of **11** and **12** (see above). Based on the formation of **13** it becomes evident that the generation of lithium amidinate **11** is not a solvent effect but represents, instead, elimination from an alkali metal zincate formed in the **10**–$ZnMe_2$–$LiBu^t$ reaction system. Further evidence for the complexity with which oxygen is scavenged by this system is provided by the isolation, from the same reaction mixture as affords **13**, of needles which are revealed by X-ray crystallography to be the heterobimetallic polymer $[(LiOBu^t)(MeZnOBu^t)_3]_\infty$ **14**. The fundamental units of these infinite chains are distorted pseudo-cubic arrangements of the type $LiZn_3O_4$ whose construction is allowed by the empirical insertion of oxygen into M–C(Bu^t) bonds (Fig. 4 and Table 3). While such behaviour is plainly analogous to that which achieves the *tert*-butoxide moiety in the distorted octahedral complex $Bu^t(\mu_3\text{-}O)Li_3(\mu_6\text{-}O)Zn_3[N(2\text{-}C_5H_4N)Me]_6$ **9**, the retention of unreacted ZnMe groups in **14** contrasts with the ZnOMe fragments noted in **12** and reveals a close relationship with the recently reported pseudo-cubic structure of $[THF \cdot Li(Bu^t)OZn(OBu^t)Me]_2$ **8**.[27] Whereas both Zn2 and Zn3 (in **14**) refine with 100% zinc occupancy, the third metal site refines with 50% Zn and 50% Li occupancy and satisfies the $LiZn_3O_4$ cluster core necessary for charge balance. This stoichiometry is borne out by the ^1H NMR spectroscopic observation of two types of *tert*-butoxy group at δ 1.28 and 1.27 in a 1 : 3 ratio. In the solid state, the methyl group involved in polymerisation (C1) occupies a crystallographic centre of symmetry midway between Li1/Zn1 and its symmetry equivalent, thus bridging between an alkali metal centre in one psuedo-cubane and a zinc centre in the adjacent one and making it impossible to distinguish unambiguously between Zn–CH_3···Li and Li–CH_3···Zn bonding modes. The dual process of site disorder and polymerisation gives rise to significant distortions in the tetranuclear units (Table 3). The pseudo-cubic array once again reveals μ_3-oxygen bonded Li–Zn triangulated arrays incorporating mono-capping of two $LiZn_2$ groups (*e.g.*, Li1Li1AZn3) and two $Li_{0.5}Zn_{2.5}$ groups (*e.g.*, Li1AZn2Zn3). Lastly, contrary to the structure of **8**,[27] that of **14** reveals longer interactions between bridging oxygen and metal centres with lithium character; the (μ_3-O2A)Li1AZn2Zn3 moieties reveal Li–O and Zn–O distances of 2.078(3) Å and 2.066 Å (mean), respectively.

Conclusions

The structures of the alkoxy and oxide complexes **12**, **13** and **14** point to a predilection for oxo-capped triangulated metal arrays in oxgenated Li–Zn systems incorporating *N,N′*-diphenylbenzamidinate ligands and establishes some generality for the motifs described recently to result from the comparable treatment of similar 2-pyridylanilide systems.[27] Moreover, a close relationship is revealed between those complexes (obtained using P_2O_5 dried air) and the ones reported here which are afforded by the action of O_2. The empirical insertion of oxygen into a Zn–Me bond is revealed by the structure of dimeric **12** (*cf.* both **5** and **7**). Obtained concomitantly with the polymeric alkoxide co-complex **14**, oxide-encapsulation complex **13** reveals two mono-capped Li_2Zn triangles fused at O^{2-}, with the ligand orientations about the metallooxide core bearing a marked relationship to those in dimer **12**. Lastly, the pseudo-cubic building blocks of **14** highlight the selective reactivity of labile M–C bonds towards oxygen (*cf.* **8**). All of the structures reported here point to the processes active during oxygenation being non-trivial. Moreover, it is clear that systems such as those considered here are capable of generating several products concomitantly. Accordingly, mechanistic studies are ongoing. These are focussed on the multinuclear NMR spectroscopic analysis of reaction mixtures and specific complexes and also attempts to isolate and fully characterise other reaction intermediates and products. The results of these investigations will be reported subsequently.

Experimental

Methods and materials

All reactions and manipulations were carried out under an inert atmosphere of dry nitrogen, using standard double manifold and glove-box techniques. Where appropriate the treatment of air-sensitive reaction mixtures with oxygen was achieved using molecular oxygen (BOC) dried over P_2O_5 (Lancaster). All other chemical reagents were used as received from Aldrich or Lancaster without further purification. Toluene and THF were distilled off sodium or sodium–potassium amalgam immediately prior to use.

NMR data were collected on either a Bruker DPX 400 or DRX 400 (400.12 MHz for ^1H) or a Bruker DRX 500 FT NMR

Table 4 Crystallographic details for **12**·PhMe·2THF, **13**·2PhMe and **14**

	12·PhMe·2THF	**13**·2PhMe	**14**
Formula	$C_{101}H_{106}Li_2N_8O_6Zn_2$	$C_{128}H_{106}Li_4N_{12}OZn_2$	$C_{19}H_{45}LiO_4Zn_3$
M	1672.56	1986.75	540.60
T/K	180(2)	180(2)	180(2)
Radiation, λ/Å	Mo-Kα, 0.7107	Mo-Kα, 0.7107	Mo-Kα, 0.7107
Crystal system	Triclinic	Monoclinic	Orthorhombic
Space group	$P\bar{1}$	$C2/c$	$Pnma$
a/Å	12.5676(6)	17.4711(5)	19.9640(10)
b/Å	13.3855(7)	24.7419(8)	12.6772(6)
c/Å	15.8867(8)	24.2561(7)	11.2548(3)
α/°	107.555(2)	90	90
β/°	94.761(2)	90.718(2)	90
γ/°	115.412(3)	90	90
V/Å^3	2230.39(19)	10484.3(5)	2848.5(2)
Z	1	4	4
ρ_{calc}/g cm^{-3}	1.245	1.259	1.261
μ/mm^{-1}	0.596	0.516	2.522
θ_{max}/°	25.04	22.46	27.48
Measured refl.	18047	23899	14315
Independent refl.	7796	6712	3387
R_{int}	0.0626	0.0848	0.0761
T_{min}, T_{max}	0.953, 0.971	0.788, 0.921	0.729, 0.882
S	1.030	1.030	1.068
$R1$ [$I > 2\sigma(I)$]	0.0566	0.0657	0.0500
$wR2$ (all data)	0.1421	0.1794	0.1528

spectrometer (500.05 MHz for ^{1}H) at 27 °C. Chemical shifts are quoted relative to TMS.

Synthesis and characterisation

Synthesis of [THF·Li(Me)OZnAm$_2$]$_2$, 12. ZnMe$_2$ (0.5 ml, 1 mmol, 2.0 M in toluene) was added to a solution of *N,N′*-diphenylbenzamidine (**10**, 0.27 g, 1 mmol) in toluene (2 ml). After reaction had ceased the yellow solution was chilled to −78 °C and Bu^{t}Li (0.59 ml, 1 mmol, 1.7 M in pentane) was added. The resultant mixture was returned to room temperature and treated with O$_2$ (*ca.* 15 s). The addition of THF (1 ml) led to solvation when the mixture was refluxed. Filtration and room temperature storage for 24 hours resulted in the deposition of colourless crystals of **12**. Yield 123 mg (32%) (by **10** consumed), mp decomp. from 218 °C. Found: C 71.92, H 6.64, N 7.03%. Calc. for $C_{101}H_{106}Li_2N_8O_6Zn_2$: C 72.57, H 6.35, N 6.71%. ^{1}H NMR spectroscopy (500 MHz, CD$_3$CN): δ 7.26–5.82 (m, 65H, Ph + *Ph*Me), 3.77–3.70 (m, 6H, OMe), 3.65 (m, 13H, THF), 2.34 (s, 3H, Ph*Me*), 1.81 (m, 13H, THF), 1.28 (s, 3H, by-product), 1.19–1.18 (m, 6H, by-product).

Co-synthesis of (μ_6-O)(Li$_2$ZnAm$_3$)$_2$ 13 and [(LiOBu^t)(MeZnOBu^t)$_3$]$_\infty$ 14. ZnMe$_2$ (0.5 ml, 1 mmol, 2.0 M in toluene) was added to a slurry of *N,N′*-diphenylbenzamidine (**10**, 0.27 g, 1 mmol) in toluene (10 ml) at −78 °C. The mixture was allowed to warm to room temperature whereupon it was stirred for 10 minutes before being returned to −78 °C. Bu^{t}Li (0.59 ml, 1 mmol, 1.7 M in pentane) was added and the resultant white suspension left to attain ambient temperature. Treatment of the suspension with O$_2$ (*ca.* 15 s) and reflux afforded a yellow solution which deposited a mixture of colourless blocks (**13**) and needles (**14**) upon storage at room temperature for 24 hours. These could be mechanically separated for the purposes of analysis.

For **13**: Yield 40 mg (34%) (by **10** consumed), mp decomp. from 252 °C. Found: C 73.75, H 5.99, N 9.27%. Calc. for $C_{128}H_{106}Li_4N_{12}OZn_2$: C 77.38, H 5.38, N 8.46%. ^{1}H NMR spectroscopy (500 MHz, CD$_3$CN): δ 7.74–6.68 (m, br, 95H, Ph + *Ph*Me), 2.33 (s, 3H, Ph*Me*), 1.18 (s, 2H, trace Bu^t from **14**), −0.45 (s, 0.5H, trace Me from **14**).

For **14**: Yield 51 mg (38%) (by Bu^{t}Li consumed), mp >350 °C. Found: C 43.61, H 7.92%. Calc. for $C_{19}H_{45}LiO_4Zn_3$: C 42.21, H 8.39%. ^{1}H NMR spectroscopy (400 MHz, CD$_3$CN): δ 1.28 (s, 3H, Bu^{t}OLi), 1.27 (s, 9H, Bu^{t}OZn), −0.63 (s, 3H, MeZn).

X-Ray crystallography

Data for **12**·PhMe·2THF, **13**·2PhMe and **14** were collected using a Nonius Kappa CCD diffractometer equipped with an Oxford Cryostream low-temperature device (Table 4). Structures were solved by direct methods using SIR-92[49] and refined against F^2 using SHELXL-97.[50] Hydrogen atoms were placed geometrically and allowed to ride during subsequent refinement. In the case of **13**·2PhMe, crystals were found to diffract relatively weakly and data were observed only to $2\theta = 22.5°$ (equivalent to 0.93 Å resolution).

CCDC reference numbers 168577–168579.

See http://www.rsc.org/suppdata/dt/b1/b104444n/ for crystallographic data in CIF or other electronic format.

For **12**·PhMe·2THF, the THF solvent molecule was found to be disordered and was modelled in two orientations with refined occupancies 70 : 30%. In neither orientation was it possible to distinguish the oxygen atom from the CH$_2$ groups and the atomic sites in the 5-membered rings were modelled, therefore, as 80% CH$_2$: 20% O. In **13**·2PhMe, each metal site was modelled initially as 100% Zn and refined with an isotropic displacement parameter. For Zn1 and Zn2, the resulting values of U_{iso} were significantly larger than those for the other two Zn sites, suggesting less electron density to be present at the latter sites. This observation, together with the requirement for charge balance, is consistent with one lithium centre being disordered over the two metal sites. The disorder was modelled, therefore, as Li1 and Zn1 coincident at the first metal site and Li2 and Zn2 coincident at the second metal site. The occupancies of Li1, Zn1, Li2 and Zn2 were refined with the constraints sof(Li1) + sof(Zn1) = 100%, sof(Li2) + sof(Zn2) = 100% and sof(Li1) + sof(Li2) = 100%, and with isotropic displacement parameters fixed at 0.05 Å^2. This step converged to give 42% Li1 : 58% Zn1 and 58% Li2 : 42% Zn2. The occupancies were fixed to these values during subsequent refinement and the metal sites were then refined with an isotropic displacement parameter common to Li1, Li2, Zn1 and Zn2. The toluene molecules in **13**·2PhMe were observed to be disordered and were modelled in two equally-occupied orientations. Treatment of the metal sites in **14** was identical to that in **13**·2PhMe; Zn2 and Zn3 were refined satisfactorily with 100% zinc occupancy while U_{iso} for Zn1 suggested some degree of lithium occupancy at this site. The requirement for charge balance in **14** necessitates exactly one lithium per three zinc centres, constraining the occupancies at the mixed-metal site to 50% Li1 : 50%

Zn1. The bridging methyl group (C1) occupies a crystallographic centre of symmetry midway between the Zn1/Li1 site and its symmetry equivalent. Thus, the methyl group bridges Li1 and Zn1 in adjacent molecular units but the crystallographic disorder prohibits absolute discrimination of the two arrangements Zn–$CH_3 \cdots$ Li and Li–$CH_3 \cdots$ Zn.

Acknowledgements

We thank the UK EPSRC for financial support (A. D. B., D. J. L., P. S.) and for financial assistance with purchase of the CCD diffractometers.

References

1 M. Fieser, *Fieser & Fieser's Reagents for Organic Synthesis: Vol. 17*, John Wiley & Sons Inc., New York, 1994, pp. 161–173 and 207–227; *Encyclopedia of Reagents for Organic Synthesis: Vol. 5*, Ed.-in-chief L. A. Paquette, John Wiley & Sons Ltd., Chichester, 1995, pp. 2968–3188; T.-L. Ho, *Fiesers' Reagents for Organic Synthesis: Vol. 18*, John Wiley & Sons Inc., New York, 1999, pp. 204–223 and 257–263.

2 D. Linton, P. Schooler and A. E. H. Wheatley, *Coord. Chem. Rev.*, 2001, **223**, 53.

3 D. J. Ager, I. Fleming and S. K. Patel, *J. Chem. Soc., Perkin Trans. 1*, 1981, 2520.

4 R. A. N. C. Crump, I. Fleming and C. J. Urch, *J. Chem. Soc., Perkin Trans. 1*, 1994, 701.

5 B. Weidmann and D. Seebach, *Angew. Chem., Int. Ed. Engl.*, 1983, **22**, 31; M. T. Reetz, *Angew. Chem., Int. Ed. Engl.*, 1984, **23**, 556.

6 M. Kitamura, S. Okada, S. Suga and R. Noyori, *J. Am. Chem. Soc.*, 1989, **111**, 4028; S. Niwa and K. Soai, *J. Chem. Soc., Perkin Trans. 1*, 1991, 2717; M. Nakamura and E. Nakamura, *J. Am. Chem. Soc.*, 1993, **115**, 11016; M. Yamakawa and R. Noyori, *J. Am. Chem. Soc.*, 1995, **117**, 6327; M. Kitamura, M. Yamakawa, H. Oka, S. Suga and R. Noyori, *Chem. Eur. J.*, 1996, **2**, 1173.

7 E. Negishi and K. Akiyoshi, *J. Am. Chem. Soc.*, 1988, **110**, 646; P. Kocienski, S. Wadman and K. Cooper, *J. Am. Chem. Soc.*, 1989, **111**, 2363; E. Negishi, K. Akiyoshi, B. O'Conner, K. Takagi and G. Wu, *J. Am. Chem. Soc.*, 1989, **111**, 3089; P. Knochel, T.-S. Chou, H. G. Chen, M. C. P. Yeh and M. J. Rozema, *J. Org. Chem.*, 1989, **54**, 5202; P. Knochel, N. Jeong, M. J. Rozema and M. C. P. Yeh, *J. Am. Chem. Soc.*, 1989, **111**, 6474; M. J. Rozema and P. Knochel, *Tetrahedron Lett.*, 1991, **32**, 1855.

8 Y. Kondo, N. Takazawa, C. Yamazaki and T. Sakamoto, *J. Org. Chem.*, 1994, **59**, 4717; Y. Kondo, N. Takazawa, A. Yoshida and T. Sakamoto, *J. Chem. Soc., Perkin Trans. 1*, 1995, 1207; Y. Kondo, T. Matsudaira, J. Sato, N. Murata and T. Sakamoto, *Angew. Chem., Int. Ed. Engl.*, 1996, **35**, 736; Y. Kondo, M. Fujinami, M. Uchiyama and T. Sakamoto, *J. Chem. Soc., Perkin Trans. 1*, 1997, 799.

9 T. Harada, K. Katsuhira, K. Hattori and A. Oku, *J. Org. Chem.*, 1993, **58**, 2958.

10 M. Uchiyama, M. Koike, M. Kameda, Y. Kondo and T. Sakamoto, *J. Am. Chem. Soc.*, 1996, **118**, 8733.

11 M. Uchiyama, Y. Kondo, T. Miura and T. Sakamoto, *J. Am. Chem. Soc.*, 1997, **119**, 12372; M. Uchiyama, M. Kameda, O. Mishima, N. Yokoyama, M. Koike, Y. Kondo and T. Sakamoto, *J. Am. Chem. Soc.*, 1998, **120**, 4934.

12 E. Weiss and H. Plass, *J. Organomet. Chem.*, 1968, **14**, 21.

13 M. Westerhausen, B. Rademacher and W. Schwarz, *Z. Anorg. Allg. Chem.*, 1993, **619**, 675.

14 M. Westerhausen, M. Wieneke, W. Ponikwar, H. Nöth and W. Schwarz, *Organometallics*, 1998, **17**, 1438.

15 M. Westerhausen, B. Radmacher, W. Schwarz and S. Henkel, *Z. Naturforsch, Teil B*, 1994, **49**, 199.

16 E. Rijnberg, J. T. B. H. Jastrzebski, J. Boersma, H. Kooijman, N. Veldman, A. L. Spek and G. van Koten, *Organometallics*, 1997, **16**, 2239.

17 H.-O. Fröhlich, B. Kosan, B. Undeutsch and H. Görls, *J. Organomet. Chem.*, 1994, **472**, 1.

18 A. J. Edwards, A. Fallaize, P. R. Raithby, M.-A. Rennie, A. Steiner, K. L. Verhorevoort and D. S. Wright, *J. Chem. Soc., Dalton Trans.*, 1996, 133.

19 R. Wyrwa, H.-O. Fröhlich and H. Görls, *Organometallics*, 1996, **15**, 2833.

20 W. Clegg, P. A. Hunt and B. P. Straughan, *Acta Crystallogr., Sect. C*, 1993, **49**, 2109.

21 G. C. Forbes, A. R. Kennedy, R. E. Mulvey, R. B. Rowlings, W. Clegg, S. T. Liddle and C. C. Wilson, *Chem. Commun.*, 2000, 1759.

22 A. R. Kennedy, R. E. Mulvey and R. B. Rowlings, *Angew. Chem., Int. Ed.*, 1998, **37**, 3180.

23 A. R. Kennedy, R. E. Mulvey and R. B. Rowlings, *J. Am. Chem. Soc.*, 1998, **120**, 7816.

24 A. R. Kennedy, R. E. Mulvey, C. L. Raston, B. A. Roberts and R. B. Rowlings, *Chem. Commun.*, 1999, 353.

25 R. P. Davies, D. J. Linton, R. Snaith and A. E. H. Wheatley, *Chem. Commun.*, 2000, 193; D. R. Armstrong, R. P. Davies, D. J. Linton, P. Schooler, G. P. Shields, R. Snaith and A. E. H. Wheatley, *J. Chem. Soc., Dalton Trans.*, 2000, 4304.

26 R. P. Davies, D. J. Linton, R. Snaith and A. E. H. Wheatley, *Chem. Commun.*, 2000, 1819.

27 R. P. Davies, D. J. Linton, P. Schooler, R. Snaith and A. E. H. Wheatley, *Chem. Eur. J.*, 2001, **7**, 3696.

28 H. Bock, T. Hauck, C. Näther, N. Rösch, M. Staufer and O. D. Häberlen, *Angew. Chem., Int. Ed. Engl.*, 1995, **34**, 1353.

29 For the Main Group organometallic derivitisation of benzamidines see: R. P. Davies, D. J. Linton, P. Schooler, R. Snaith and A. E. H. Wheatley, *Eur. J. Inorg. Chem.*, 2001, 619 and refs. cited therein.

30 I. Cragg-Hine, M. G. Davidson, F. S. Mair, P. R. Raithby and R. Snaith, *J. Chem. Soc., Dalton Trans.*, 1993, 2423; J. Barker, D. Barr, N. D. R. Barnett, W. Clegg, I. Cragg-Hine, M. G. Davidson, R. P. Davies, S. M. Hodgson, J. A. K. Howard, M. Kilner, C. W. Lehmann, I. Lopez-Solera, R. E. Mulvey, P. R. Raithby and R. Snaith, *J. Chem. Soc., Dalton Trans.*, 1997, 951.

31 J. Jubb, S. Gambarotta, R. Duchateau and J. H. Teuben, *J. Chem. Soc., Chem. Commun.*, 1994, 2641; H. C. Aspinall and M. R. Tillotson, *Inorg. Chem.*, 1996, **35**, 2163.

32 W. J. Evans, R. Dominguez and T. P. Hanusa, *Organometallics*, 1986, **5**, 1291.

33 T. Dubé, S. Conoci, S. Gambarotta and G. P. A. Yap, *Organometallics*, 2000, **19**, 1182.

34 J. Jubb and S. Gambarotta, *J. Am. Chem. Soc.*, 1993, **115**, 10410; J. Jubb and S. Gambarotta, *Inorg. Chem.*, 1994, **33**, 2503.

35 A. Kasani, R. P. K. Babu, K. Feghali, S. Gambarotta, G. P. A. Yap, L. K. Thompson and R. Herbst-Irmer, *Chem. Eur. J.*, 1999, **5**, 577.

36 A. E. H. Wheatley, unpublished work.

37 R. E. Mulvey, *Chem. Soc. Rev.*, 1998, **27**, 339.

38 F. M. Mackenzie, R. E. Mulvey, W. Clegg and L. Horsburgh, *Polyhedron*, 1998, **17**, 993; F. A. Cotton, L. M. Daniels, C. A. Murillo and H.-C. Zhou, *C. R. Acad. Sci. Ser. IIc*, 1999, **2**, 577.

39 H. Dietrich and D. Rewicki, *J. Organomet. Chem.*, 1981, **205**, 281; H.-J. Gais, J. Vollhardt, H. Günther, D. Moskau, H. J. Lindner and S. Braun, *J. Am. Chem. Soc.*, 1988, **110**, 978; S. C. Ball, I. Cragg-Hine, M. G. Davidson, R. P. Davies, M. I. Lopez-Solera, P. R. Raithby, D. Reed, R. Snaith and E. M. Vogl, *J. Chem. Soc., Chem. Commun.*, 1995, 2147; W. Clegg, L. Horsburgh, P. R. Dennison, F. M. Mackenzie and R. E. Mulvey, *Chem. Commun.*, 1996, 1065; J. F. K. Müller, M. Neuburger and M. Zehnder, *Helv. Chim. Acta*, 1997, **80**, 2182; T. Chivers, A. Downard and G. P. A. Yap, *J. Chem. Soc., Dalton Trans.*, 1998, 2603; J. F. K. Müller, M. Neuburger and B. Spingler, *Angew. Chem., Int. Ed.*, 1999, **38**, 3549.

40 M. Driess, H. Pritzkow, S. Martin, S. Rell, D. Fenske and G. Baum, *Angew. Chem., Int. Ed. Engl.*, 1996, **35**, 986; M. Driess, U. Hoffmanns, S. Martin, K. Merz and H. Pritzkow, *Angew. Chem., Int. Ed.*, 1999, **38**, 2733.

41 R. H. Heyn, J. C. Hufman and K. G. Caulton, *New J. Chem.*, 1993, **17**, 797.

42 T. M. Che, V. W. Day, L. C. Francesconi, M. F. Fredrich, W. G. Klemperer and W. Shum, *Inorg. Chem.*, 1985, **24**, 4055.

43 P. Miele, J. D. Foulon, N. Hovnanian and L. Cot, *J. Chem. Soc., Chem. Commun.*, 1993, 29; P. Miele, G. Foulon and N. Hovnanian, *Inorg. Chim. Acta*, 1997, **255**, 289.

44 J. L. Jolas, S. Hoppe and K. H. Whitmire, *Inorg. Chem.*, 1997, **36**, 3335.

45 M. Baier, P. Bissinger, J. Blümel and H. Schmidbaur, *Chem. Ber.*, 1993, **126**, 947.

46 M. Veith, E.-C. Yu and V. Huch, *Chem. Eur. J.*, 1995, **1**, 26.

47 R. Schmid, A. Mosset and J. Galy, *Inorg. Chim. Acta*, 1991, **179**, 167.

48 B. A. Vaartstra, W. E. Streib and K. G. Caulton, *J. Am. Chem. Soc.*, 1990, **112**, 8593; W. J. Evans, M. A. Ansari and J. W. Ziller, *Inorg. Chem.*, 1999, **38**, 1160.

49 A. Altomare, G. Cascarano, C. Giacovazzo and A. Guargliardi, *J. Appl. Crystallogr.*, 1993, **26**, 343.

50 G. M. Sheldrick, SHELXL-97, Program for Crystal Structure Refinement, University of Göttingen, Germany, 1997.